Nonlinear Inferential Cascade Control of Exothermic Fixed-Bed Reactors

Xiangming Hua and Arthur Jutan
Dept. of Chemical and Biochemical Engineering, University of Western Ontario, London, Ontario N6A 5B9, Canada

A nonlinear inferential cascade control strategy for a tubular fixed-bed reactor with highly exothermic reaction is presented. Tight control of exit conversion and stabilization of hot-spot temperature was achieved over a wide range of operating conditions. A multiple cascade structure was developed by lumping the distributed-parameter system and partitioning it into three subsystems. Practical issues of implementing the control system are addressed, as well as physical insight and assumptions used for model reduction of each subsystem. The direct synthesis approach for nonlinear control systems is used to design the controllers of the important subsystems separately. A lag was added in the primary subsystem, and fast stabilization of the secondary subsystem was implemented. Unknown temperature states and inlet concentration were estimated by a nonlinear observer from only a few temperature measurements. The control problem of the moving hot-spot temperature was also addressed. Simulation on an industrial phthalic anhydride fixed-bed reactor showed that the observer can give excellent dynamic tracking of the reactor. The resulting cascade control system can achieve good set-point tracking and disturbance rejection performance, which is robust in the presence of measurement error and model mismatch, and superior to a single-loop control system.

Introduction

Fixed-bed reactors (FBRs) usually function as the heart of process industries. However, in practice, fixed-bed reactors are still often not under closed-loop control, or have only indirect control, such as via hot-spot temperature, for the primary controlled variables. The controller design for the fixed-bed reactor may be considerably complicated by several intricate characteristics: (1) extreme nonlinearity; (2) distributed-parameter systems; (3) the stiff character of the system model resulting from very different time scales of the internal physical and chemical processes; (4) uncertain or time-varying parameters; (5) constraints on manipulated and state variables; (6) limited on-line measurement information. Moreover, for tubular fixed-bed reactors with exothermic reactions, which are widely used for processing industries, it is necessary to control simultaneously peak temperature and exit concentration (or conversion), which is a primary controlled variable, for preventing bed temperature from being excessive and achieving operation goals. In spite of this knowledge, the reported studies concerning the control of fixed-bed reactors have been traditionally based on a local linearized model (Jutan et al., 1977; Jørgensen and Jensen, 1990). However, linear controllers can yield satisfactory performance, only if the plant is operated in a small range around a nominal steady state. The fixed-bed reactor may be subject to large disturbances or significant set point changes from an on-line optimizer. Therefore, it is important to develop and implement nonlinear control strategies for fixed-bed reactors to allow tight operation of both controlled variables available over a wide range of conditions.

In recent years, significant progress has been made in the development of nonlinear model-based controller design methods. There are a lot of reported successful applications of new nonlinear control methods, such as feedback linearization techniques based on differential geometric theory and generic model control (GMC) (Lee and Sullivan, 1988; Kravaris and Kantor, 1990; Bequette, 1990). GMC, which is a

Correspondence concerning this article should be addressed to A. Jutan.

direct synthesis approach (Ogunnaike and Ray, 1994), is developed with the specific objective of incorporating the nonlinear process model directly in the control algorithm, and is relatively easy to apply from a practical point of view. However, many applications of these nonlinear control techniques are limited to some relatively simple process systems, such as continuous or batch stirred tank chemical reactors, biochemical reactors, and polymerization reactors. So far, only a few applications are concerned with studies on applications of these techniques to complex process systems (Doyle III et al., 1997). In fact, there are a number of restrictions and constraints encountered in applying these techniques to complex distributed-parameter systems like fixed-bed reactors. One of them is that the control synthesis techniques require relatively low-order nonlinear lumped-parameter models. Recently, Doyle III et al. (1997) proposed a nonlinear control methodology for a fixed-bed reactor with exothermic reaction, which is a two-tier approach: (*i*) develop a low-order wave propagation model; (*ii*) synthesize a feedback linearizing control law for the hot-spot temperature control of the reactor. However, it is not easy to develop a quantitatively accurate low-order wave propagation model for the fixed-bed reactor. Also, the control of the hot-spot temperature is usually only an indirect control for the fixed-bed reactor.

The effectiveness of cascade control in allowing improvement of control performance of nonlinear lumped-parameter systems, such as CSTR, has been well established (Chidambaram and Yugendar, 1992; Liu and Macchietto, 1995). Moreover, the introduction of the cascade structure provides some opportunities to reduce process uncertainty, and static and dynamic interaction. Through investigation of physical characteristics and a detailed mechanistic model of the fixed-bed reactor with exothermic reactions, we find that a cascade structure is very helpful for handling the above difficult characteristics and achieving the control objective. Under the cascade structure, the control of both the exit conversion (or exit concentration) and the hot-spot temperature can be achieved. Instead of dealing with the entire system, the cascade structure allows the design of a controller for each subsystem separately. Portions of the system are often easier to handle than the entire one since their model size is much smaller. It is thus possible to apply nonlinear control techniques for the controller design of each subsystem, depending on different characteristics and control requirements. In practice, on-line measurement of whole temperature and concentration profiles along the reactor is often not available, except for a few temperature measurements and off-line concentration samplings at the reactor inlet/exit. In this case, it is necessary to estimate the unknown temperature states and infer the exit concentration, or exit conversion. Nevertheless, with the cascade structure, the inferential control can improve reliability of the closed-loop control system (Budman et al., 1992). Therefore, a nonlinear inferential cascade control strategy for exothermic fixed-bed reactors based on system partitioning is presented. Due to other benefits of using the cascade structure, the resultant nonlinear inferential cascade control scheme for the fixed-bed reactor can be expected to create improved control performance.

To implement this scheme for the fixed-bed reactor, some practical issues should be addressed. Unlike classical cascade control systems, there are here some special features, which result in difficult design problems. At first, the issue of a distributed-parameter process must be addressed. Since there is strong interaction between the subsystems, and, in addition, the primary subsystem has much faster dynamics than the secondary one, a technique to separate partially the dynamics of the subsystems is required. The main disturbance inlet concentration is unknown, and affects not only the secondary subsystem, but also the primary one; therefore, estimation and rejection of the inlet concentration, which is usually a very difficult task in control of the fixed-bed reactor, must be addressed. Furthermore, the temperature profile along the reactor may move as some inlet conditions change, and so the control problem of the moving hot-spot temperature has to be dealt with. In addition, estimation of unknown states and output, and update of the time-varying physical parameter, may be also required.

A mechanistic dynamic model that describes the behavior of the fixed-bed reactor with exothermic reactions is given, and a suitable lumped model is developed by the orthogonal collocation method (OCM). A multiple cascade structure with three subsystems is developed by a partitioning-space approach. The model reduction of each subsystem by making use of physical insight and some reasonable assumptions is presented. Then, a nonlinear inferential cascade control scheme is proposed. The direct synthesis approach for nonlinear control systems is used to design the controller for the primary and secondary subsystems, and the PID technique for the third subsystem. A lag is added in the primary subsystem, and fast stabilization of the secondary subsystem is implemented. Two different control schemes with fixed and moving hot-spot positions are developed. An estimation approach of unknown states and inlet disturbance using a nonlinear observer (Zeitz, 1977; Hua et al., 1998) is presented. Other issues, such as output inference and parameter update, are also discussed. To demonstrate the efficiency of the resultant control strategy, closed-loop simulation studies on a commercial-scale fixed-bed reactor for phthalic anhydride synthesis (Chen and Sun, 1991) in the Matlab/Simulink environment are carried out, and the results are discussed.

Reactor Model

First-principle model

In order to achieve effective model-based control and optimization of the fixed-bed reactor, the development of a first-principle model, which gives a full description of the internal laws of the reactor, has received considerable attention in both academia and industry. The propensity to use a rigorous full model for fixed-bed reactor control has also been enhanced by increased computing power at reduced costs. So far, many rigorous models of fixed-bed reactors are available (Froment, 1967; Hua et al., 1998), and some of them have been collected and coded in standard simulation libraries such as ASPEN and DIVA (Kroener et al., 1990). Figure 1 shows a typical tubular fixed-bed reactor, used with exothermic reactions. Simulation and experimented results show that their steady and dynamic behavior can be well described by the following dimensionless, coupled, nonlinear PDEs, in which a pseudo-homogeneous assumption is made, radial gradients are properly approximated, and axial diffusion of reactants, wall capacity, and heat loss of reactor are neglected.

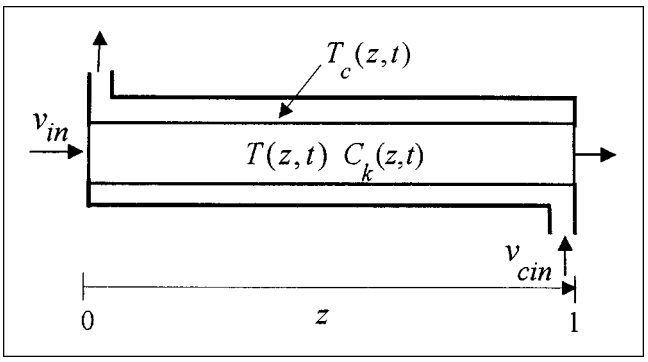

Figure 1. Exothermic fixed-bed reactor.

$k = 1, \cdots, m$.

Mass balance

$$\epsilon\frac{\partial C_k}{\partial t} = -\frac{\partial C_k}{\partial z} + \mu(1-\epsilon)Da\bar{R}_k\left(\bar{C},T,\bar{\gamma}\right) \qquad (1)$$

Energy balance in the catalytic bed

$$Le\frac{\partial T}{\partial t} = -\frac{\partial T}{\partial z} + \frac{1}{Pe_h}\frac{\partial^2 T}{\partial z^2} + \mu(1-\epsilon)\beta Da\sum_{k'=1}^{p}(-\Delta H_{k'})R_{k'}(C_{k'},T,\gamma_{k'}) + \alpha(T_c - T) \qquad (2)$$

Energy balance in the jacket

$$\frac{\partial T_c}{\partial t} = \tau_c\frac{\partial T_c}{\partial z} + \Omega_c(T - T_c) \qquad (3)$$

and boundary conditions

at $z = 0$: $C_k = C_{k,\text{in}}$, $T = T_{\text{in}}$,

at $z = 1$: $T_c = T_{c,\text{in}}$, $\dfrac{\partial T}{\partial z} = 0$.

where

$$k = 1, \cdots, m; \quad \bar{C} = [C_1 \cdots C_m]^T, \quad \bar{\gamma} = [\gamma_1 \cdots \gamma_p]^T.$$

The definitions of some main dimensionless, normalized model parameters are given in Appendix A.

This kind of catalytic fixed-bed reactor with highly exothermic reactions, is one of the processes that is the most difficult to control in chemical engineering, because of the complex steady and dynamic characteristics. A typical feature of the temperature profile along the reactor is that there is a peak (or hot-spot) temperature, as shown in Figure 2. In industrial practice, this hot-spot temperature is traditionally considered as a controlled variable. Although control of the temperature at a position alone cannot ensure the regulation of the entire temperature profile at a desired profile, it can be justified from the standpoint that it allows prevention of excessive bed temperature caused by unknown disturbances. However, such indirect control does not ensure the regulation of exit conversion at its desired target value.

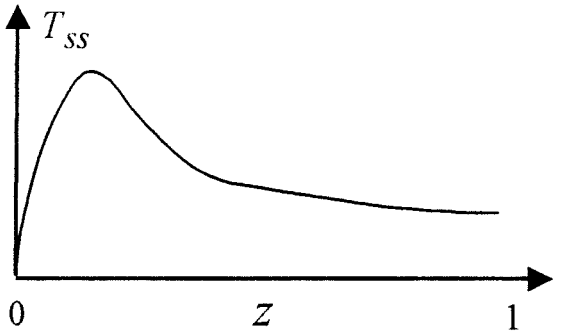

Figure 2. Typical steady-state temperature profile.

Lumping model via OCM

For control purposes, lumping of the distributed first-principle model is required. A traditional approach is to lump using the orthogonal collocation method (OCM) (Finlayson, 1972). By some straightforward algebraic manipulations, Eqs. 1–3 are converted to the following $(m+2)\times(n+1)$ nonlinear ODEs

$$\frac{dC_{k,i}}{dt} = \frac{1}{\epsilon}\left\{-\sum_{j=0}^{n+1}A_{i,j}C_{k,j} + \mu(1-\epsilon)Da\bar{R}_{k,i}\left(\bar{C}_i,T_i,\bar{\gamma}\right)\right\} \qquad (4)$$

$$\frac{dT_i}{dt} = -\tau\sum_{j=0}^{n+1}A_{i,j}T_j + \lambda\sum_{j=0}^{n+1}B_{i,j}T_j + \mu(1-\epsilon)\sum_{k'=1}^{p}\Psi_{k'}R_{k',i}(C_{k',i},T_i,\gamma_{k'}) + \Omega(T_{ci} - T_i) \qquad (5)$$

$$\frac{dT_{ci}}{dt} = \tau_c\sum_{j=0}^{n+1}A_{i,j}T_{cj} + \Omega_c(T_i - T_{ci}) \qquad (6)$$

where $C_{k,i} = C_k(z_i,t)$, $k = 1, \cdots, m$; $T_i = T(z_i,t)$; $T_{ci} = T_c(z_i,t)$, $i = 1, \cdots, n+1$; n is the number of interior collocation points along the reactor length, which are chosen as the roots of shifted Legendre orthogonal polynomials. $A_{i,j}$ and $B_{i,j}$ $(i,j = 0, \cdots, n+1)$ are elements of collocation matrices (Finlayson, 1972). The other model parameters such as τ, λ, $\Psi_{k'}$ and Ω can be easily obtained from the model (Eqs. 1–3). The number of collocation points n has to be chosen to make the order of the lumped model as low as possible while keeping the model errors in prescribed bounds.

Partitioning and Model Reduction

Unfortunately, the entire lumped model (Eqs. 4–6) is usually difficult to be directly used for designing a nonlinear controller for the fixed-bed reactor. The model is often too large.

Moreover, the model is very stiff because of significantly different time scales between concentration and temperature changes in the fixed-bed reactor. However, from some physical considerations, we can show that this system (Eqs. 4–6) permits a multiple cascade structure. With the above control objective, we select coolant flow rate or jacket inlet temperature as the manipulated variable, and exit conversion (or exit concentration) as the primary controlled variable (output). Also, we select some state variables as intermediate outputs. Using system partitioning, the entire system can be structured as a cascade system. Because portions of the system are often easier to handle than the the entire one, this approach provides a new possible way to design a nonlinear controller for such a complex system.

Partitioning of system

There are different methods that can be used to partition a nonlinear system. The suggested methods are only available for nonlinear lumped-parameter systems. Some researchers partitioned a system by a direct approach based on the physical knowledge of the system (Kozub et al., 1987; Windes and Ray, 1992; Chidambaram and Yugendar, 1992). Liu and Macchietto (1995) presented a partitioning-space approach for partitioning a general nonlinear SISO system into two subsystems. One of its advantages is that the required conditions for partitioning a system are easy to check. Moreover, this approach provides a theoretical justification for the particular decomposition of the nonlinear system. However, for our system (Eqs. 4–6), more than two subsystems have to be dealt with, and the intermediate outputs to be selected may not be just a pure state variable, but a function of the state vector, because of, for example, the movement of the hot-spot position. Therefore, their concept needs to be extended for partitioning our system.

Let

$$C = \left[C_1^T \cdots C_m^T \right]^T;\ C_k = \left[C_{k1} \cdots C_{k(n+1)} \right]^T,\ (k = 1,\ \ldots,\ m) \tag{7}$$

$$T = \left[T_1 \cdots T_{n+1} \right]^T \tag{8}$$

$$T_c = \left[T_{c1} \cdots T_{c(n+1)} \right]^T \tag{9}$$

$$X = \left[C^T T^T T_c^T \right]^T \tag{10}$$

The model (Eqs. 4–6) can be rewritten in the following vector form

$$\dot{C} = f_{\mathrm{I}}(X) + s_{\mathrm{I}}(X)d \tag{11}$$

$$\dot{T} = f_{\mathrm{II}}(X) + s_{\mathrm{II}}(X)d \tag{12}$$

$$\dot{T}_c = f_{\mathrm{III}}(X) + g_{\mathrm{III}}(X)u + s_{\mathrm{III}}(X)d \tag{13}$$

$$y = h(X) \tag{14}$$

where, f, s and g are nonlinear function vectors with suitable dimensions; h is a nonlinear function; u, y and d are scalar control input, output, and disturbance. Here, the control input u is chosen as coolant inlet temperature, or coolant flow rate. The reactant feed flow rate is constrained by upstream or downstream units, and usually regulated to a constant value. Usually, the inlet concentration is an unknown disturbance due to unpredictable changes of reactant feed concentration and difficulty of concentration measurement. The inlet temperature may be often regulated separately, because its changes result in the movement of the hot-spot position. If this is not the case, the inlet temperature can be considered as a known disturbance. It is easy to extend the following results to the case with a disturbance vector. It should be pointed out that the inlet temperature is not considered here as a manipulated variable to control the hot-spot temperature, since it may exhibit an inverse response to changes in inlet temperature. The output y is exit concentration or conversion, and thus is a function of only C. Because it is the primary output, Eq. 14 can be defined as

$$y \triangleq y_{\mathrm{I}} = h_{\mathrm{I}}(C) \tag{15}$$

In order to partition this system, we should select two new intermediate outputs. Because the hot-spot temperature is usually selected as an important indirect controlled variable in industrial practice, it should be one candidate. Another intermediate output is chosen as the coolant temperature, since it is traditionally used for servo control of the hot-spot temperature. From the practical point of view, there may be two cases. That is, when the hot-spot position is essentially fixed, we can select

Case 1 (Fixed hot-spot position).

$$y_{\mathrm{II}} = T_h \in T \tag{16}$$

$$y_{\mathrm{III}} = T_{\mathrm{cr}} \in T_c \tag{17}$$

where T_h, which is here a state in T, stands for a temperature at or near the hot-spot position, and T_{cr}, which is here a state in T_c, is a representative coolant temperature. With this choice, we find that the following conditions are satisfied

$$\frac{\partial f_{\mathrm{I}j}}{\partial T_h} \neq 0,\ f_{\mathrm{I}j} \in f_{\mathrm{I}} \tag{18}$$

$$\frac{\partial h_{\mathrm{I}}}{\partial C}\left(\frac{\partial f_{\mathrm{I}}}{\partial T_h} + \frac{\partial s_{\mathrm{I}}}{\partial T_h} \right) \neq 0 \tag{19}$$

and

$$\frac{\partial f_{\mathrm{II}j}}{\partial T_{\mathrm{cr}}} \neq 0,\ f_{\mathrm{II}j} \in f_{\mathrm{II}} \tag{20}$$

$$\frac{\partial h_{\mathrm{II}}}{\partial T}\left(\frac{\partial f_{\mathrm{II}}}{\partial T_{\mathrm{cr}}} + \frac{\partial s_{\mathrm{II}}}{\partial T_{\mathrm{cr}}} \right) \neq 0 \tag{21}$$

Thus, according to the partitioning-space concept proposed by Liu and Macchietto (1995), the system (Eqs. 11–14) can be

partitioned as

Subsys I: $$\dot{C} = f_{\mathrm{I}}(X, T_h) + s_{\mathrm{I}}(X)d \tag{22a}$$

$$y_{\mathrm{I}} = h_{\mathrm{I}}(C) \tag{22b}$$

Subsys II: $$\dot{T} = f_{\mathrm{II}}(X, T_{\mathrm{cr}}) + s_{\mathrm{II}}(X)d \tag{23a}$$

$$y_{\mathrm{II}} = T_h \tag{23b}$$

Subsys III: $$\dot{T}_c = f_{\mathrm{III}}(X) + g_{\mathrm{III}}(X)u + s_{\mathrm{III}}(X)d \tag{24a}$$

$$y_{\mathrm{III}} = T_{\mathrm{cr}}. \tag{24b}$$

However, the hot-spot position may move along the reactor length. The representative coolant temperature may be considered as a temperature at some position along the jacket length, or an average value of some coolant temperatures, such as the inlet and outlet temperatures in jacket. Here we assume that the T_h^* and T_{cr}^* are nonlinear functions of T and T_c, respectively. Thus, we could have another intermediate outputs as well

Case 2 (Moving hot-spot position)

$$y_{\mathrm{II}} = h_{\mathrm{II}}(T) \triangleq T_h^* \tag{25}$$

$$y_{\mathrm{III}} = h_{\mathrm{III}}(T_c) \triangleq T_{\mathrm{cr}}^* \tag{26}$$

Using this choice, and if $h_{\mathrm{II}}(T)$ and $h_{\mathrm{III}}(T_c)$ have continuous derivatives of order one, the following conditions exist

$$\frac{\partial f_{\mathrm{I}j}}{\partial T_h^*} \neq 0,\ f_{\mathrm{I}j} \in f_{\mathrm{I}} \tag{27}$$

$$\frac{\partial h_{\mathrm{I}}}{\partial C}\left(\frac{\partial f_{\mathrm{I}}}{\partial T_h^*} + \frac{\partial s_{\mathrm{I}}}{\partial T_h^*}\right) \neq 0 \tag{28}$$

and

$$\frac{\partial f_{\mathrm{II}j}}{\partial T_{\mathrm{cr}}^*} \neq 0,\ f_{\mathrm{II}j} \in f_{\mathrm{II}} \tag{29}$$

$$\frac{\partial h_{\mathrm{II}}}{\partial T}\left(\frac{\partial f_{\mathrm{II}}}{\partial T_{\mathrm{cr}}^*} + \frac{\partial s_{\mathrm{II}}}{\partial T_{\mathrm{cr}}^*}\right) \neq 0. \tag{30}$$

Thus, the system (Eqs. 11–14) can be partitioned for case 2 as

Subsys I: $$\dot{C} = f_{\mathrm{I}}(X, T_h^*) + s_{\mathrm{I}}(X)d \tag{31a}$$

$$y_{\mathrm{I}} = h_{\mathrm{I}}(C) \tag{31b}$$

Subsys II: $$\dot{T} = f_{\mathrm{II}}(X, T_{\mathrm{cr}}^*) + s_{\mathrm{II}}(X)d \tag{32a}$$

$$y_{\mathrm{II}} = T_h^* \tag{32b}$$

Subsys III: $$\dot{T}_c = f_{\mathrm{III}}(X) + g_{\mathrm{III}}(X)u + s_{\mathrm{III}}(X)d \tag{33a}$$

$$y_{\mathrm{III}} = T_{\mathrm{cr}}^* \tag{33b}$$

Model reduction of subsystems

Due to the complex behavior of the fixed-bed reactor, there are strong interactions between these subsystems. In order to implement a control system based on the partitioned system, it is necessary to reduce the models of subsystems. The model reduction for the entire system is usually more difficult. Here, because of the availability of a partitioned system, it is possible to reduce the model based on the characteristics and control requirements of each subsystem. Because of the similarity of the approach, only model reduction of the subsystem (Eqs. 22–24) is discussed.

For the fixed-bed reactor, it is noted that some physical insight can be used for reducing the model of Subsystem I. Because the concentration of all reactants in a catalytic bed may dynamically change more than 1,000 times faster than the bed temperature, the concentration can be considered to be at a quasi-steady state. In addition, for a strong oxidation reaction, the reaction kinetics can be approximated to be pseudo-first-order due to the large excess of oxygen. Furthermore, it could be assumed that

(a) the reaction rate terms in Eqs. 1–3 are separable, that is,

$$R_k(C,T) = \xi_{c,k}(C)\xi_{T,k}(T)$$

where ξ_c and ξ_T are functions of only concentration and temperature, respectively;

(b) both concentration and temperature have finite values, or $C_{k,\min} \leq \| C_k \| \leq C_{k,\max}$ and $T_{\min} \leq \| T \| \leq T_{\max}$.

For example, when considering a reaction system $A \rightarrow B \rightarrow C$, let C_a be the concentration of component A. Its reaction rate can be expressed as an Arrhenius form

$$R_a(C_a,T) = \varphi_{a0} \exp\left(-\frac{\gamma_a}{T}\right) C_a$$

where φ and γ are parameters, which are related to frequency factor and activation energy, respectively. The above assumptions cause Eq. 4 to be represented by the following algebraic equation

$$C_a = G_a(T)\, pC_{\mathrm{ain}} \tag{34}$$

where $C_a = [C_{a1} \cdots C_{a(n+1)}]^T$, G_a is a $(n+1)\times(n+1)$ nonlinear function matrix

$$G_a(T) = \left[-A + \mathrm{diag}\left\{\mu(1-\epsilon)\,Da\varphi_{a0}\exp\left(-\frac{\gamma_a}{T_i}\right)\right\}\right]^{-1},$$
$$i = 1, \ldots, (n+1) \tag{35}$$

in which A is the collocation matrix. According the above assumption (b), the inverse of matrix in the right of Eq. 35 exists. p is a $(n+1)\times 1$ vector. In addition, the exit conversion can be defined as

$$y_p = \frac{C_{\mathrm{ain}} - C_{a(n+1)}}{C_{\mathrm{ain}}} \tag{36}$$

Therefore, the model (Eqs. 22a–22b) can be represented as

$$\textbf{Subsys I:}\quad C_a = G_a(T,T_h)\,pC_{\text{ain}} \tag{37}$$

$$y_{\text{I}} = y_p \tag{38}$$

Similarly, under the above assumptions, all C_k ($k=1, \ldots m$) can also be approximated by appropriate expressions which are functions of T, and thus the concentration variables in Eq. 23a can be eliminated. Therefore, we get the reduced model of Subsystem II

$$\textbf{Subsys II:}\quad \dot{T} = \Phi(T) + bT_{\text{cr}} + \Gamma(T)C_{\text{ain}} \tag{39}$$

$$y_{\text{II}} = T_h \tag{40}$$

where Φ, Γ are $(n+1)\times 1$ nonlinear function vectors, and b are a $(n+1)\times 1$ vector.

In practice, the control of coolant temperature is often made relatively simple. In fact, by simulating the behavior of the reactor, it is found that the jacket can reasonably be approximated to be a lumped-parameter system. It reflects the fact that the jacket is assumed to be well mixed. The coolant is usually chosen as a very large heat capacity material, such as cooling oil, and can be considered to be thermally unaffected by the contents of the reactor. Thus, the coolant temperature profile along the jacket length can be eliminated, and instead only a temperature at a position along the jacket or an average one could be considered. Therefore, the dynamics of the Subsystem III can be approximated by a first-order ODE

$$\textbf{Subsys III:}\quad \dot{T}_{\text{cr}} = a_c T_{\text{cr}} + b_c u \tag{41}$$

$$y_{\text{III}} = T_{\text{cr}}. \tag{42}$$

where a_c, b_c are constant parameters to be identified.

It should be pointed out that the above reduction approach can be used for the case when the reaction kinetics is not first-order, if some approximations to the concentration expression $\xi_c(C)$ in the reaction kinetics can be made. In addition, some other nonlinear model reduction approaches can also be used for the model reduction of the above subsystems, such as developing a low-order wave propagation model for the Subsystem II (Doyle III et al., 1997).

Cascade Control System Design

Based on the above partitioning of the system, a multiple cascade control structure is developed by considering T_h (or T_h^*) and T_{cr} (or T_{cr}^*) as intermediate control inputs for Subsystem I and Subsystem II, respectively, as shown in Figure 3. Under this structure, the control objectives of the fixed-bed reactor can be achieved. The control of the exit conversion (or exit concentration) can be achieved through the primary controller. The control of the hot-spot temperature can be dealt with as a stabilization problem. This can be achieved by designing a proper secondary controller which is required to reach efficient servo control of T_h. Such a cascade control structure can accommodate various standard or nonlinear

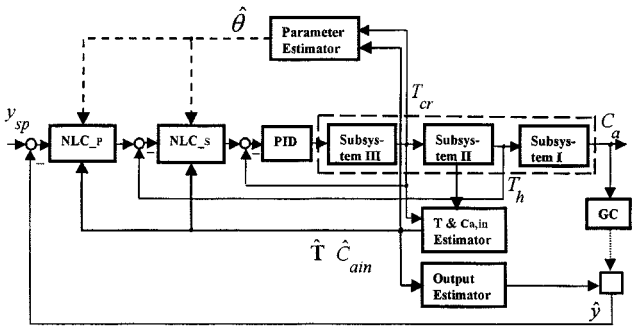

Figure 3. Cascade control system.

control techniques in each subsystem. Since the controller for each subsystem can be designed separately, it is possible to select a suitable control technique for different subsystems, depending on the characteristics and the control requirements of the specific subsystem. In our case, as mentioned above, the dynamics of the third subsystem is relatively simple. Moreover, this loop aims mainly to achieve servo control of T_{cr}. Therefore, we design a conventional PID controller for the third subsystem. It should be noted that the closed-loop bandwidth of the third loop must be designed to be greater than that of the secondary one so as to dynamically decouple the two loops.

Because of their complexity, more attention should be paid to the design of the primary and the secondary controllers. Their designs are strongly affected by the complex nonlinear dynamics of these subsystems, and the important control objectives of the fixed-bed reactor. Furthermore, unlike classical cascade control systems, there are some unusually difficult features in the present system. The dynamics of the primary subsystem is at quasi-steady state, and thus is much faster than that of the secondary one. The hot-spot temperature may move as some inlet conditions change. The disturbance of unknown inlet concentration enters not only the secondary subsystem, but also the primary one. Also, all temperature states along the reactor length are often not measurable. Therefore, we use nonlinear control techniques to design these controllers, and develop an inferential cascade control system, as shown in Figure 3. The part blocked in the longest broken line represents the partitioned system. The **NLC_p** and **NLC_s** stand for the primary and secondary nonlinear controllers, respectively. The solid line stands for on-line, the broken one for off-line, or the signal with a relatively large sampling interval. In addition, this figure also contains several estimators, such as state and disturbance, and output estimator, which will be discussed in the next section. A dynamic output compensator is included in Figure 3 with the attempt to compensate for the estimated output using the sampling data of the outlet concentration measured by a gas chromatographic (GC) device. This is not directly used for the feedback control since it has a relatively slow sampling rate. Therefore, this is a nonlinear inferential cascade control system.

Direct synthesis approach of nonlinear controller design

Some existing nonlinear control techniques can be applied for the design of the **NLC_p** and **NLC_s**. Here, we propose

using a direct synthesis approach (Ogunnaike and Ray, 1994). The approach is developed with the specific objective of incorporating the nonlinear process model directly in the control algorithm. The generic model control (GMC) presented by Lee and Sullivan (1988) is such an approach. If the relative order of the process is one, GMC is equivalent to GLC (global input/output linearization controller). The formulation of the GMC controller is relatively straightforward, and its tuning is simple. Importantly, this approach has several advantages that are desirable for designing control systems of the fixed-bed reactor:

(a) The nonlinear (reduced) process model is directly incorporated in the control algorithm, allowing for the inherent nonlinearity of the fixed-bed reactor to be taken into account;

(b) Tedious (even difficult) algebraic manipulations for control laws due to the complex reduced model of subsystems, which may occur when using, for example, the feedback linearization technique based on differential geometric theory, are avoided;

(c) Feedforward control action is explicitly included in the control algorithm;

(d) Some difficult design issues in the cascade control system of the fixed-bed reactor can be handled, since the basic GMC method can be extended, for example, to allow for a steady-state model to be used and for the incorporation of process constraints.

Assume that a given real process can be described by following SISO nonlinear equation

$$\dot{x} = f(x, u, d) \tag{43}$$

$$y = h(x) \tag{44}$$

where x is a $N\times 1$ state vector; u, d, and y are scalar input, disturbance, and output, respectively. f and h are a $N\times 1$ nonlinear function vector and nonlinear function, respectively. According to the GMC basic principle (Lee and Sullivan, 1988), we can get the control algorithm which consists of three terms (with dynamic process model, proportional action term and integral action term, respectively)

$$\hat{H}_x \hat{f}(x,u,d) - K_1(y_{\rm sp} - y) - K_2\int_0^t (y_{\rm sp} - y)\,dt = 0 \tag{45}$$

where $\hat{H}_x = \partial\hat{h}/\partial x$, $\hat{f}$ and $\hat{h}$ represent the approximation to the true model (Eqs. 43 and 44), K_1 and K_2 are tuning parameters, and $y_{\rm sp}$ is the set point of the output. The control law (Eq. 45) directly imbeds an approximate dynamic nonlinear model. Through tuning the controller, reasonable closed-loop performance specification can be achieved. Any mismatch between the predicted behavior from the model and the real process will be compensated for by the integral term. This term insures not only robust behavior in the presence of model error, but also the elimination of steady-state offset. However, for fast stabilization control, it may not be wise to use too much integral action.

In order to implement the cascade control system, some connective steps in designing both the primary and secondary controllers by the GMC technique should be followed. To partially separate the dynamics between the primary loop and the secondary loop, we propose adding a lag in the primary loop, and doing fast stabilization in the secondary loop. Since the GMC algorithm provides the nonlinear feedforward action, the disturbances entered into both the primary and secondary loops can effectively be rejected. Different cases, with fixed and moving hot-spot positions, require accommodation in each of their respective subsystems.

Design of NLC_s

When the movement of hot-spot position is negligible, the **NLC_s** can be designed based on the reduced model (Eqs. 39–40) of Subsystem II. In this case, $y_{\rm II}$ can be expressed as

$$y_{\rm II} = T_h = c^T T \tag{46}$$

where $c^T = [0\cdots 1\ 0\cdots 0]$ is a $1\times(n+1)$ vector, in which the element 1 corresponds to the state at or near the hot-spot position. Thus, the GMC control algorithm of **NLC_s** can be obtained based on the Subsystem II

$$T_{\rm cr,sp} = [c^T b]^{-1}\Big\{ - c^T[\Phi(T) + \Gamma(T)C_{\rm ain}] + K_{s1}e + K_{s2}\int_0^t e dt\Big\} \tag{47}$$

where the output of **NLC_s** is the set point of the third loop, and thus represented by $T_{\rm cr,sp}$, $e = T_{h,\rm sp} - T_h$, K_{s1} and K_{s2} are tuning parameters of **NLC_s**.

When the hot-spot position is moving, a modification of the control algorithm is required. If the hot-spot temperature can be expressed by Eq. 25, the GMC control algorithm of **NLC_s** is

$$T_{\rm cr,sp} = \left[\frac{\partial h_{\rm II}}{\partial T} b\right]^{-1}\Big\{ - \frac{\partial h_{\rm II}}{\partial T}[\Phi(T) + \Gamma(T)C_{\rm ain}] + K_{s1}e + K_{s2}\int_0^t e dt\Big\}. \tag{48}$$

However, in practice, it is difficult to get an analytic mathematical expression (Eq. 25) of T for the hot-spot temperature. Here, we propose the following procedure: first, estimate the hot-spot temperature T_h (or the maximum temperature) based on T by, for example, the interpolating technique, and then implement the control law

$$T_{\rm cr,sp} = b_h^{-1}\left[- \Phi_h(T_h) - \Gamma_h(T_h)C_{\rm ain} + K_{s1}e + K_{s2}\int_0^t e dt\right] \tag{49}$$

where b_h, Φ_h, and Γ_h can be obtained from the model (Eq. 39).

It can be noted that the output of the above GMC controller can be explicitly represented, because the subsystem II has a control affine form. Implementation of such control algorithms is straightforward.

Design of NLC_p

Since the reduced model (Eq. 37) of Subsystem I has a steady-state form, the above basic GMC method cannot be directly used for designing the **NLC_p**. Cott et al. (1989) proposed an extension of GMC for steady-state models by introducing some estimate of the process dynamic response. In our case, the problem is more complicated, because the primary loop is much faster than the secondary loop, which is very poor practice for cascade control. Therefore, it is necessary to decouple the dynamics between the two loops. There are some methods to solve this problem. For example, Bramilla and Semino (1992) introduced a nonlinear filter between the two controllers. Here, we propose to augment the model of the Subsystem I with a simple lag. Thus, the dynamics of the two loops can be properly separated by tuning the parameter of the lag. Moreover, such a combined process model can be used for designing a GMC controller for the primary loop. Through some algebraic manipulations to the model (Eqs. 37–38), the output of Subsystem I can be expressed as

$$y_{\mathrm{I}} = w(T, T_h, C_{\mathrm{ain}}) \tag{50}$$

where w is a nonlinear function. When the lag $1/(\tau_p s + 1)$ (τ_p is a tuning parameter) is added, we get

$$\dot{y} = \frac{1}{\tau_p}\left[w(T, T_h, C_{\mathrm{ain}}) - y \right] \tag{51}$$

According to the GMC principle, the control algorithm of **NLC_p** can be developed based on the model (Eq. 51)

$$-\frac{1}{\tau_p}\left[w(T, T_{h,\mathrm{sp}}, C_{\mathrm{ain}}) - y \right] + K_{p1} e + K_{p2} \int_0^t e dt = 0 \tag{52}$$

where $e = y_{\mathrm{sp}} - y$, y_{sp} represents the set point for exit conversion (exit concentration); K_{p1} and K_{p2} are tuning parameters of **NLC_p**. Since the output of the **NLC_p** is the set point of T_h, we use $T_{h,\mathrm{sp}}$ to represent it. When the hot-spot position is moving, the control algorithm (Eq. 52) should be appropriately modified. In addition, since the control algorithm is implicit in $T_{h,\mathrm{sp}}$, it requires some iterative numerical method for solving.

State (Disturbance) and Primary Output Estimation

The implementation of the control system of the fixed-bed reactor requires some knowledge such as concentration and temperature profiles along the reactor. In industrial practice, there may be only some off-line samplings of concentration at the reactor inlet/exit, since it could be very problematic to measure the concentration on-line. Although, in some cases, concentration analyzers such as a GC device are installed, they are usually expensive to operate and maintain, and have relatively slow sampling rates. In addition, the reactors may be built with just a few temperature measurement points. Therefore, it is necessary to estimate unknown temperature states at some collocation points, inlet concentration (main disturbance), and output concentration (related to primary output) on-line. In this work, the partitioning of the system facilitates the estimation of the unknown states, output and model parameters, and even the disturbances of the fixed-bed reactor. Here, we will implement these estimators based on the reduced models.

Estimation of state and disturbance

Due to the availability of the reduced model, there are some approaches to estimate the unknown states, such as the extended Kalman filter. Generally, a more difficult task is to estimate the disturbance, inlet concentration, particularly for the fixed-bed reactor. Several alternative ways are possible for estimating the disturbance of a process, but they are empirical approaches, and often applied to lumped-parameter processes such as the CSTR. Two factors are important for insuring convergence and accuracy of the estimate: how to appropriately structure the unknown disturbance and how to estimate it. Here, we present a combined state and disturbance estimation approach to estimate the unknown temperature states and inlet concentration. We set the inlet concentration C_{ain} as a new state variable in an extended system, and then design a nonlinear state observer.

Considering the common practice in industry, we assume that the unknown inlet concentration can be described by a simple disturbance model

$$\dot{C}_{\mathrm{ain}} = \zeta(t); \qquad \zeta(0) = C_{a0} \tag{53}$$

where $\zeta(t)$ is assumed to be an unknown, but bounded function. Some researchers employed $\zeta(t) = 0$ for disturbance estimation, or assumed a constant inlet concentration in some small time interval. Combining the reduced model (Eq. 39) and the disturbance model (Eq. 53), we have the following extended state model for estimation problem

$$\dot{T} = \Phi(T) + bT_{\mathrm{cr}} + \Gamma(T) C_{\mathrm{ain}} \tag{54}$$

$$\dot{C}_{\mathrm{ain}} = \zeta(t) \tag{55}$$

$$Y = c^T T \tag{56}$$

where Y stands for a temperature measurement vector.

There are many studies on nonlinear observers, but the available results are problem-dependent, suitable for a very restricted class of nonlinear systems (Soroush, 1997). For the estimation problem of the Eqs. 54–56, some theoretical results about, for example, the observability and convergence of such an observer problem have been presented. And, also, some researchers developed nonlinear observers (Farza et al., 1997). When $\zeta = 0$, some researchers showed that the estimation error converges exponentially to zero (Deza et al., 1992). Here according to the common practice in the industrial fixed-bed reactor, we assume $\zeta = 0$, and use an extended Luenberger observer

$$\dot{\hat{T}} = \Phi(\hat{T}) + bT_{\mathrm{cr}} + \Gamma(\hat{T})\hat{C}_{\mathrm{ain}} + L_1(Y - \hat{Y}) \tag{57}$$

$$\dot{\hat{C}}_{\mathrm{ain}} = L_2(Y - \hat{Y}) \tag{58}$$

where L_1 and L_2 are gains of the observer. These observer gains could be nonlinear function matrices with respect to state and input variables of the observer. Then since the observer structure is fixed, the remaining problem is the choice of the gains L_1 and L_2 to meet the general requirements on an observer such as asymptotic stability and fast convergence to the real states. We adopt the Zeitz's concept (Zeitz, 1977; Hua et al., 1998) to design the observer gains, the details of which are given in Appendix B. According to this concept, the nonlinear function gain matrix can be easily designed. If the observability of the system is satisfied and the gains are properly designed, the observed states and disturbance can converge to the true ones.

Estimation of output

The output (exit concentration or conversion) can be estimated from the information about temperature and inlet concentration. Based on the reduced model (Eqs. 37–38) of Subsystem I, we propose the open-loop output estimator for exit concentration

$$\hat{y}_{p1} = c^T G_a(\hat{T})\, p\hat{C}_{\text{ain}} \tag{59}$$

or for exit conversion is

$$\hat{y}_{p2} = 1 - \frac{\hat{y}_{p1}}{\hat{C}_{\text{ain}}} \tag{60}$$

where $c^T = [0 \cdots 1]$, G_a and p are obtained from Eq. 34.

In addition, it should be pointed out that in the first-principle model of the fixed-bed reactor there are some physical parameters, such as catalyst activity and wall heat-transfer coefficients that are only approximately known or that may vary during plant operation (due to the decay of catalyst activity and fouling). It is necessary to update these model parameters to reflect these changing conditions. Since, usually, the change of these parameters is relatively slow, an off-line estimation strategy may be suitable for the parameter updating. The estimation can be based on the reduced model (Eq. 39) or its steady-state model and some measurements. Some estimation technique such as the nonlinear least-square method can be used for determining the values of the model parameters that produce the best agreement between the model and the real process.

Case Studies

In order to demonstrate the efficiency of the proposed control strategy, a commercial-scale fixed-bed reactor for phthalic anhydride synthesis (Chen and Sun, 1991) is considered as an application example. This reactor consists of 2,500 tubes with diameter 2.5 cm packed with V_2O_5 catalyst and surrounded by molten salt for cooling. The feed stream contains *o*-xylene and air, with air in great excess to avoid explosion limits and suppress the temperature rise. The reactions taking place in the reactor are one parallel and two consecutive reactions

$$C_6H_4(CH_2)_2 + 3O_2 \rightarrow C_6H_4C_2O_3 + 3H_2O \tag{61}$$

$$C_6H_4C_2O_3 + 7.5O_2 \rightarrow 8CO_2 + 2H_2O \tag{62}$$

$$C_6H_4(CH_2)_2 + 10.5O_2 \rightarrow 8CO_2 + 5H_2O \tag{63}$$

These reactions are strongly exothermic. The oxidation reaction mechanism of *o*-xylene to phthalic anhydride has been well studied, and the physical model for the phthalic anhydride reactor has also been established (Froment, 1967). Obviously, this is a reaction system with $p = 3$ and $m = 2$. Due to oxygen in excess, their dimensionless reaction rates can be expressed by

$$R_1 = k_{01} \exp\left(-\frac{\gamma_1}{T}\right) C_1 / R_{\text{ref}}$$

$$R_2 = k_{02} \exp\left(-\frac{\gamma_2}{T}\right) C_2 / R_{\text{ref}}$$

$$R_3 = k_{03} \exp\left(-\frac{\gamma_3}{T}\right) C_1 / R_{\text{ref}}$$

$$\bar{R}_1 = -R_1 - R_3$$

$$\bar{R}_2 = R_1 - R_2$$

where C_1 and C_2 are the dimensionless concentration of *o*-xylene and phthalic anhydride, respectively; R_i ($i = 1,2,3$) are the rate of the ith reaction in Eqs. 61–63. It is assumed that the axial heat conduction is negligible. Thus, under the assumptions given in Eq. 1, the detailed first principle reactor model consists of four coupled dimensionless nonlinear partial differential equations representing two material balances and two energy balances. The operating conditions and values of physical parameters of the reactor, which are the same as used in Chen and Sun (1991), are given in Table 1.

From a practical perspective, industrial fixed-bed reactors traditionally rely on tight control of coolant temperature in achieving optimal operation of the reactor. Here, it is assumed that the coolant temperature is controlled by a conventional PID technique. Also, the inlet flow rate and the inlet temperature are individually regulated to keep constant using conventional controllers. The behavior of the reactor was investigated in many steady-state and dynamic simulations based on the first principle model of the reactor. It was found that the reactor has some physical constraints on the manipulated and state variables such as 628 $K \le T_h \le 700$ K

Table 1. Values of Physical Parameters and Operating Conditions

$L = 4$ m	$\rho_f = 0.582$ kg/m^3
$\epsilon = 0.35$	$\rho_c = 1{,}851.456$ kg/m^3
$k_{01} = 2.418 \times 10^9$ 1/s	$\rho_s = 2{,}000$ kg/m^3
$k_{02} = 2.706 \times 10^9$ 1/s	$C_{pf} = 1{,}045$ J/(kg·K)
$k_{03} = 1.013 \times 10^9$ 1/s	$C_{pc} = 483.559$ J/(kg·K)
$E_1 = 1.129 \times 10^5$ J/mol	$C_{ps} = 836.0$ J/(kg·K)
$E_2 = 1.313 \times 10^5$ J/mol	$r_0 = 0.0125$ m
$E_3 = 1.196 \times 10^5$ J/mol	$r_1 = 0.0225$ m
$-\Delta H_1 = 1.285 \times 10^6$ J/mol	$U = 96.02$ J/(m^2·s·K)
$-\Delta H_2 = 3.276 \times 10^6$ J/mol	$C_{\text{ref}} = 0.1811$ mol/m^3
$-\Delta H_3 = 4.561 \times 10^6$ J/mol	$T_{\text{ref}} = 628.0$ K
$C^*_{1,\text{in}} = 0.1811$ mol/m^3	$v = 2.06$ m/s
$T^*_{\text{in}} = 628.0$ K	$v_c = 2.0$ m/s
$T^*_{\text{cin}} = 628.0$ K	$P = 27$–29 psig (186–200 kPa)

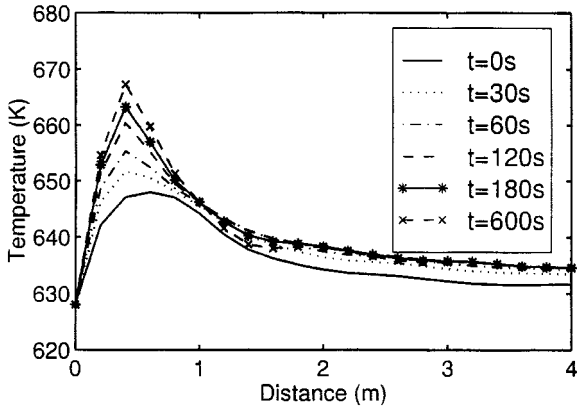

Figure 4. Temperature profiles after 4 K step increase of T_c.

and 590 K $\leq T_{cr} \leq$ 633 K. The position of the hot-spot temperature is near $z^* = 0.4$ m for the considered case. The results showed that this reactor exhibits severe nonlinearities. Figures 4–5 show dynamic temperature profiles along the reactor after a 4 K step increase and a 10 K step decrease of the representative coolant temperature, respectively.

System partitioning

The orthogonal collocation method was used to lump the first-principle model of the reactor. For the considered cases, we found that the approximation accuracy of the nonlinear lumped parameter model with six interior collocation points is sufficient. The approach of partitioning and model reduction given in the third section is applied to the above reactor system and results in 28 ODEs. According to the above assumptions, the movement of the hot-spot position could be considered negligible for this case. We consider the exit conversion of *o*-xylene as the primary output, and select two new intermediate outputs: the hot-spot temperature T_h (here, T_2 because this state is near the hot-spot position) and a representative coolant temperature T_{cr}. Such a selection of intermediate outputs satisfies the partitioning conditions (Eqs. 18–21). Therefore, through similar discussion, we get the following three subsystems

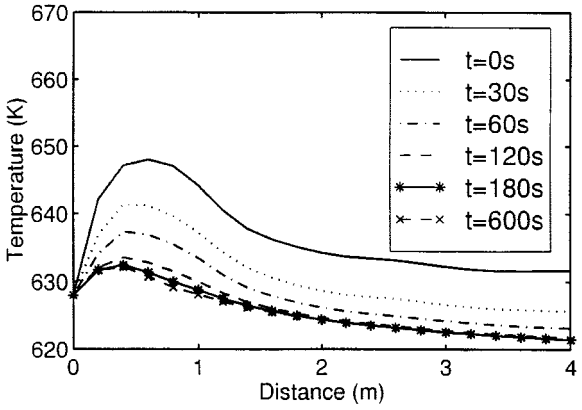

Figure 5. Temperature profiles after 10 K step decrease of T_c.

$$\textbf{Subsys I:} \quad C_1 = \Lambda(T, T_h) C_{1in} \tag{64}$$

$$y_I = y \tag{65}$$

$$\textbf{Subsys II:} \quad \dot{T} = \Phi(T) + bT_{cr} + \Gamma(T) C_{1in} \tag{66}$$

$$y_{II} = T_h \tag{67}$$

$$\textbf{Subsys III:} \quad \dot{T}_{cr} = a_c T_{cr} + b_c u \tag{68}$$

$$y_{III} = T_{cr}. \tag{69}$$

where C_1 and T are (7×1) *o*-xylene concentration and temperature state vectors, respectively Λ, Φ, Γ are (7×1) nonlinear function vectors, and b is a (7×1) vector; a_c, b_c are constant parameters to be identified.

Design of nonlinear observer

In industrial practice, usually only a few temperature measurements, such as inlet, outlet, and hot-spot temperature, are available. Therefore, unknown temperature states should be estimated to implement the control algorithms. Also, no on-line measurement of inlet and outlet concentration ($C_{1,in}$ and $C_{1,out}$) are available. Thus, we need to design one nonlinear observer (Eqs. 57–58) to estimate unknown temperature states and inlet concentration simultaneously. Once we obtain this information, the estimation of exit concentration, or conversion, is straightforward by Eq. 59 or 60.

The observer is designed based on the reduced model Eq. 66 and a measurement equation with two outputs: the hot-spot temperature (T_2) and outlet temperature (T_7). For such a nonlinear system, it is generally difficult to do the observability analysis. It depends on some factors, such as the behavior of the system and the location of measurements. To guarantee the observability of the system, at least one measurement point needs to be located in a region near the hot-spot position. Here, through checking the rank of the observability matrix of the linearized model of Eq. 66, it is found that observability conditions could be fulfilled for the above two measurement locations. The observer is designed by the approach given in Appendix B. One of the advantages of this design approach is its simplicity for tuning. Due to big difference between the dynamics of the temperature state and the inlet concentration, we should design two parts (Eq. 57 and Eq. 58) of the observer separately. Thus, the design objective becomes to determine two gains L_1 and L_2 such that the observation error asymptotically and rapidly tends to zero for various initial conditions.

This observer was tested in several nonlinear simulation studies in the case of different tuning parameters, initial observation error, random noisy measurement, and the number or location of the measurement points. Through the simulation studies, we found that for a good estimate of inlet concentration, one measurement near the hot-spot could be used. Thus, the design results in only two parameters κ_1 and κ_2 to be tuned for this observer. A reasonable choice of two parameters of the observer are $\kappa_1 = 1{,}500$ and $\kappa_2 = 50{,}000$ for the considered case. Figure 6 shows the transient behavior of the real and observed temperature states and inlet concen-

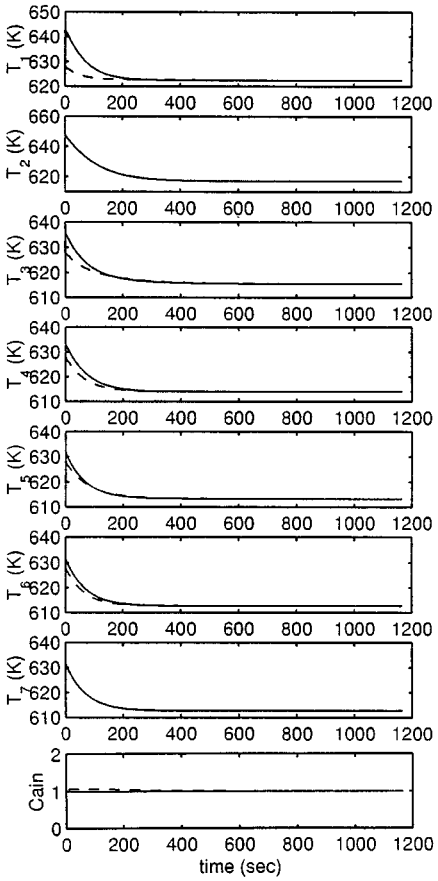

Figure 6. Transient behavior of observer with initial error: $\hat{T}_i(0) = 628.0$ K ($i = 1, \cdots, 7$) and $\hat{C}_{1,\text{in}} = 0$; and a 19 K step decrease of coolant temperature.

—— True; – – – estimate.

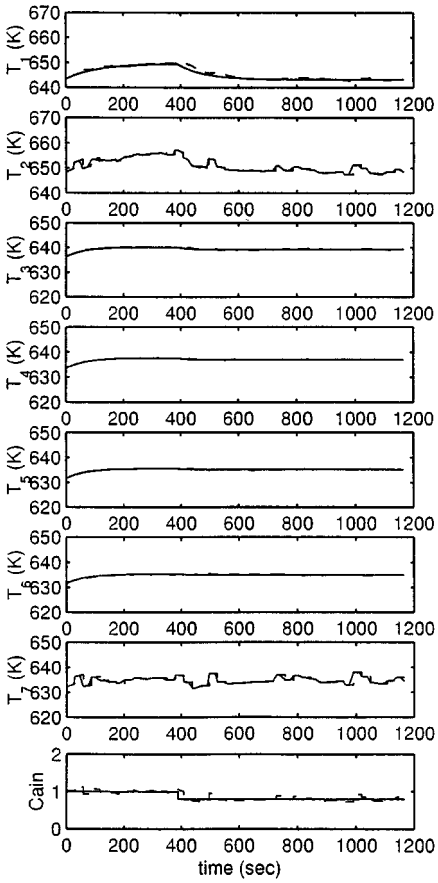

Figure 7. Transient behavior of observer with noisy measurements and after a 4.5 K step increase of coolant temperature and a 0.2 step decrease of inlet concentration near $t = 400$ s.

—— True; – – – estimate.

tration, when there is a big initial observation error due to selecting $\hat{T}_i(0) = 628.0$ K; ($i = 1, \cdots, 7$), and $\hat{C}_{1,\text{in}} = 0$; and the coolant temperature makes a 19 K step-decrease. Figure 7 illustrates the transient behavior of the real and observed temperature states and inlet concentration, when there are no initial observation errors, but noisy measurements (each temperature measurement signal is superimposed by a band-limited white noise); and the coolant temperature undergoes a 4.5 K step-increase and inlet concentration undergoes a 0.2 (or 20%) step-decrease near $t = 400$ s. From these figures, it can be found that despite various large variations for different initial conditions, the estimates of the observer rapidly converge to the real state (temperature) and disturbance (inlet concentration) of the reactor. Also, the observer is very robust against random measurement noise and the number or location of measurement points even against a large model parameter mismatch. Figure 8 gives the behavior of the observer under the same conditions as Figure 6, but a decrease in the catalyst activity from 1.0 to 0.85 (or -15%) of the reactor occurs. In this case, the estimate of temperature is still pretty good, but the estimate of inlet concentration may give a small steady-state bias.

Design of nonlinear inferential cascade control system

Based on the partitioned system, a cascade control system can be designed as discussed earlier. Because of the effectiveness of the nonlinear observer and the output estimator, they are integrated into the cascade control system to achieve a nonlinear inferential cascade control, as shown in Figure 3. In this cascade control system, we assume that the bandwidth of the third loop is designed to be larger than that of the secondary one, which implies that the PID controller can effectively track the coolant temperature set point, which is the output of the secondary controller. Obviously, the primary and secondary loops play a relatively important role in control performance. Therefore, in the following, we focus our attention on the study of the main controllers, that is, the primary and secondary controllers, of the cascade control system. Due to the physical constraints on the hot-spot and the coolant temperature, the control of the primary controller is permitted to change the set point of the secondary one by $628 \text{ K} \le T_{h,\text{sp}} \le 700$ K, and the control output of the secondary controller is permitted to change the set point of the third controller $590 \text{ K} \le T_{\text{cr,sp}} \le 633$ K. In the following, a simple ''clipping'' approach is used for the above constraint

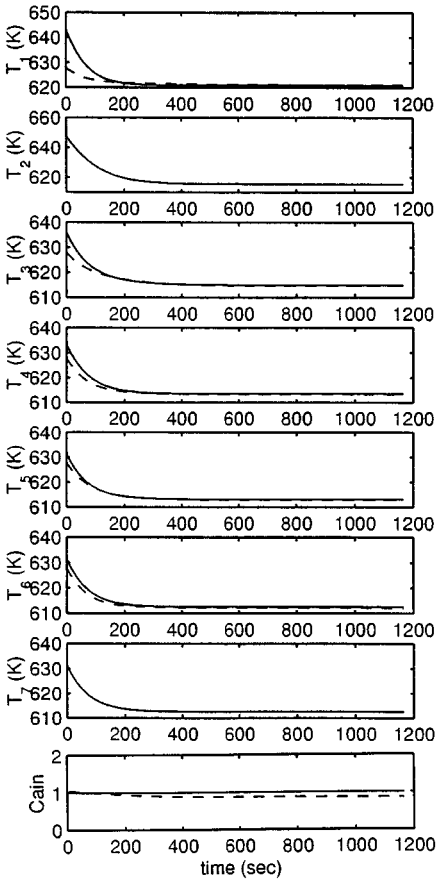

Figure 8. Transient behavior of observer with the same condition as Figure 6, although with a decrease in the catalyst activity from 1.0 to 0.85 in the reactor.

—— True; – – – estimate.

handling in the controller design. It is also assumed that the GC sampling data of inlet and outlet concentrations is not available.

As discussed in the fourth section, the GMC control is shown to have some important advantages. Therefore, although other nonlinear control techniques are available, we use the GMC technique to design the primary and secondary controllers, that is, **NLC_p** and **NLC_s** of this control system. We have shown that the GMC control algorithms of **NLC_p** and **NLC_s** can be developed based on the reduced models of Subsystem I and II, respectively. In this case, the primary controller **NLC_p** has the same control algorithm as Eq. 52, but the temperature state is estimated by the nonlinear observer and the exit conversion is obtained from the output estimator

$$-\frac{1}{\tau_p}\left[w\left(\hat{T},T_{h,\mathrm{sp}}\right)-\hat{y}\right]+K_{p1}e+K_{p2}\int_0^t e dt=0 \qquad (70)$$

where the nonlinear function w can be obtained from Eqs. 64–65; $e=y_{\mathrm{sp}}-\hat{y}$. The secondary controller **NLC_s** has the same control algorithm as Eq. 47, but the temperature state and disturbance are the estimates from the nonlinear observer

$$T_{\mathrm{cr,sp}}=\left[c^T b\right]^{-1}\left\{-c^T\left[\Phi(\hat{T})+\Gamma(\hat{T})\hat{C}_{\mathrm{ain}}\right]+K_{s1}e+K_{s2}\int_0^t e dt\right\} \qquad (71)$$

where $c^T=[0\ 1\ 0\ 0\ 0\ 0\ 0]$; b, Φ and Γ are obtained from Eqs. 66–67; $e=T_{h,\mathrm{sp}}-T_h$. In designing the above controllers, one important task is to determine the tuning parameters K_{s1}, K_{s2}, K_{p1}, K_{p2} and τ_p. To partially separate the dynamics between the two loops, the proper choice of K_{s1}, K_{s2}, and τ_p is important. Since we use GMC, it is convenient to use its tuning guide for choosing controller parameters. Since the control algorithm (Eq. 71) is explicit in the output of the controller **NLC_s**, its implementation is straightforward. However, since the control algorithm (Eq. 70) is implicit in the output of the controller **NLC_p**, an iterative numerical method should be used for solving. Here, the control Eq. 70 is solved at each control interval using a nonlinear least-squares method, that is, the Levenberg-Marquardt method. The nonlinear observer designed above is used in the inferential cascade control system. Thus, the feedforward action in the above control algorithm for rejecting the unknown disturbance (inlet concentration) can be effectively achieved. Also, the exit conversion can be inferred using the estimator (Eq. 60).

The set point tracking and disturbance rejection performance of the resulting nonlinear inferential cascade control system was investigated through many closed-loop control simulations. It was found that a reasonable choice of tuning parameters of both controllers **NLC_p** and **NLC_s** are $K_{p1}=0.01$, $K_{p2}=6.25e-6$, $\tau_p=70$, $K_{s1}=0.03$, and $K_{s2}=0$ for the considered case. Under this condition, the closed-loop control system achieves excellent set point tracking and regulation performance. Figures 9–10 depict the closed-loop control performance when the set point of exit conversion was increased by 5% to 0.9 and decreased by 10% to 0.77, respectively. In the figure, the broken lines show the set point changes of exit conversion and hot-spot temperature (calculated output of **NLC_p**), as well as the coolant temperature (calculated output of **NLC_s**), and the solid lines show the responses of the actual process. Figure 11 shows the closed-loop control performance when the inlet concentration was decreased by 20% to 0.8. To test the robustness performance of the control system, changes in process model parameters and white noise were applied to the process control simulations. Figures 12–14 show the closed-loop control performance with the same conditions as in Figures 9–10 and Figure 11, respectively, but with a decrease in the overall heat-transfer coefficient of the process by 15% from 96.02 to 81.62. When there is a decay of catalyst activity, the control performance is also very good. Figure 15 shows the closed-loop control performance when the inlet concentration was increased by 20% to 1.2, and the catalyst activity coefficient of the process was decreased by 15% to 0.85. Although the control system may not drive the process response to the set point in some cases due to the physical constraints, the system is

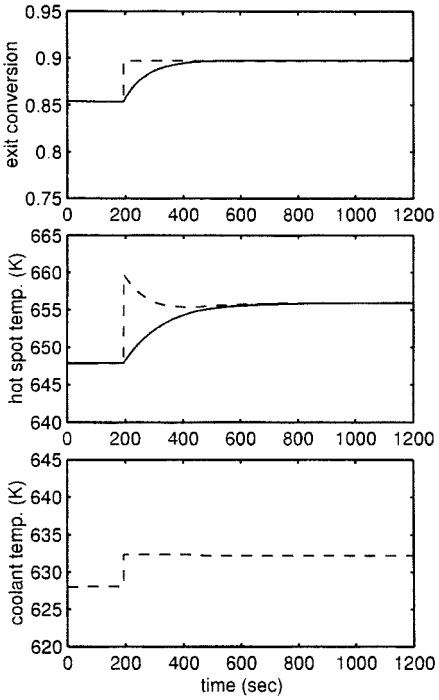

Figure 9. Control performance after a 5% step increase of exit conversion set point.

—— Response; – – – set point.

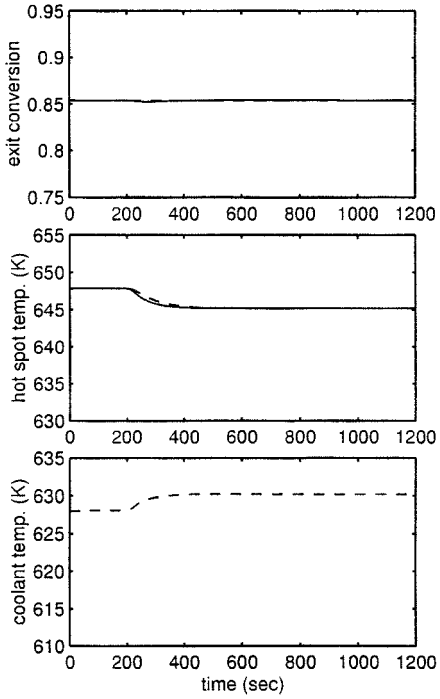

Figure 11. Control performance after a 20% step decrease of inlet concentration.

—— Response; – – – set point.

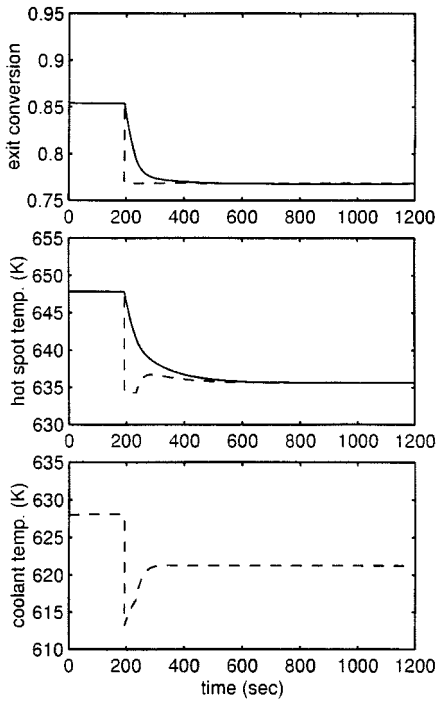

Figure 10. Control performance after a 10% step decrease of exit conversion set point.

—— Response; – – – set point.

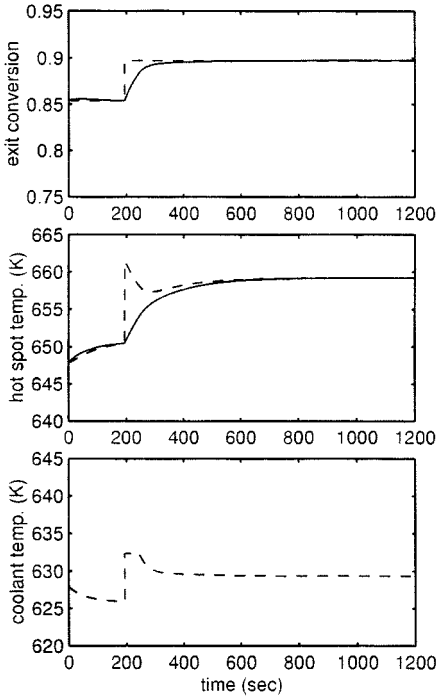

Figure 12. Control performance with the same condition as Figure 9, although with a 15% decrease in the heat-transfer coefficient of the reactor.

—— Response; – – – set point.

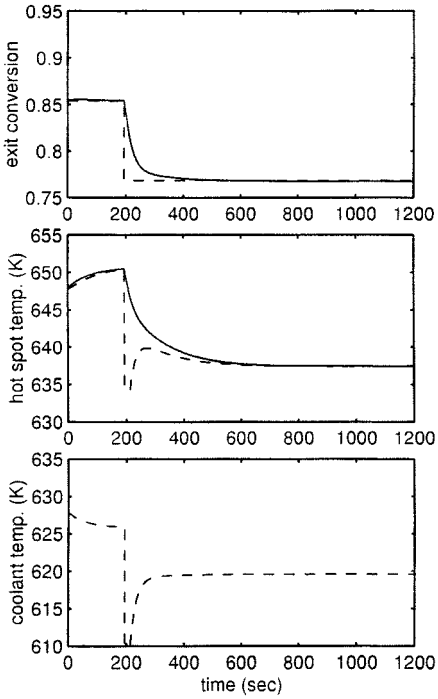

Figure 13. Control performance with the same condition as Figure 10 although with a 15% decrease in the heat-transfer coefficient of the reactor.

—— Response; – – – set point.

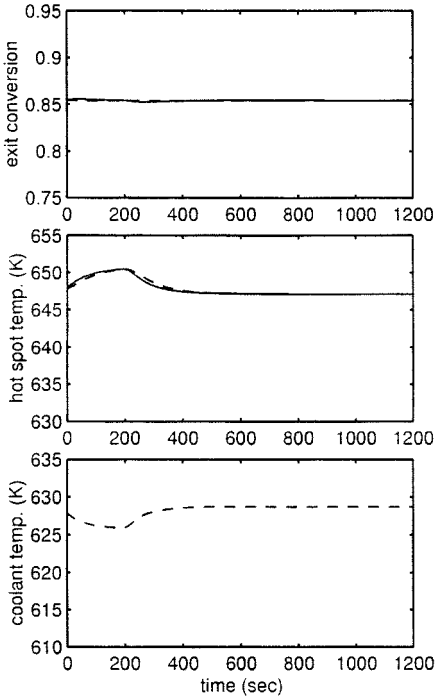

Figure 14. Control performance with the same condition as Figure 11, although with a 15% decrease in the heat-transfer coefficient of the reactor.

—— Response; – – – set point.

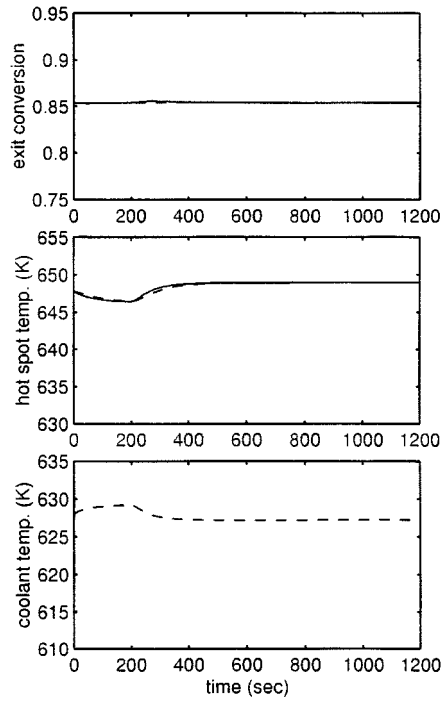

Figure 15. Control performance after a 20% step increase of inlet concentration, and a 15% decrease in the catalyst activity of the reactor.

—— Response; – – – set point.

still stable, as shown in Figure 16. This figure shows the result when the set point of exit conversion was increased by 5% to 0.9, and the catalyst activity coefficient of the process was decreased by 15% to 0.85.

Comparison with single-loop control strategy

A single-loop control strategy of exit conversion for the above fixed-bed reactor is implemented using coolant temperature as the manipulated variable. The same operating conditions and constraints on coolant temperature (590 K $\leq T_{cr} \leq$ 633 K) are employed. The nonlinear observer designed above is used to estimate the exit conversion. The adaptive generalized predictive control (GPC) (Clarke et al., 1987) is well established and has been successfully applied to the control of many nonlinear processes, and is used here to design an alternate controller. The GPC tuning parameters are set according to the guidelines of Clarke et al. (1987). In this case, the minimum costing horizon N_1, the maximum costing horizon N_2, the control costing horizon N_u and control weighting are selected as 1, 12, 1, and 0.1, respectively. In the adaptive GPC, model updating is based on a recursive least-squares parameter estimator with a forgetting factor (which is a weighting to exponentially discount older measurement information). Based on the dynamics of the open-loop behavior from coolant temperature to the estimated exit conversion, the sampling time was chosen as 30 s, and the n_a, n_b, and n_k, which are the corresponding orders and delays in the ARIMAX model, are chosen as 2, 2, and 1, respectively. The forgetting factor is 0.99. Figure 17 shows the closed-loop control result when the same change of set point (5%), as in Figure 9 is made. Due to model adaptation, even though the

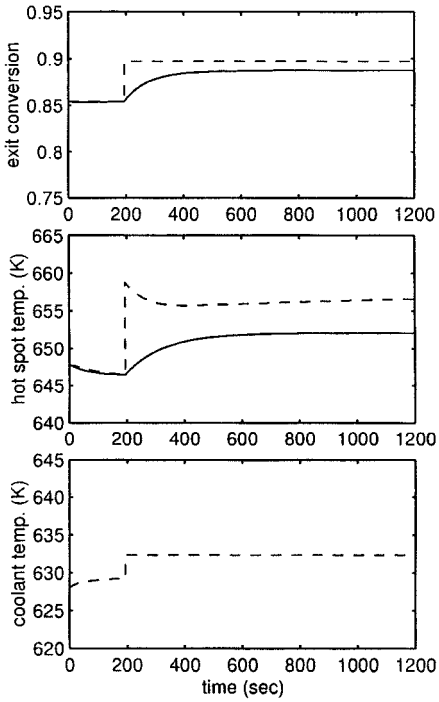

Figure 16. Control performance after a 5% step increase of exit conversion set point and a 15% decrease in the catalyst activity of the reactor.

—— Response; – – – set point.

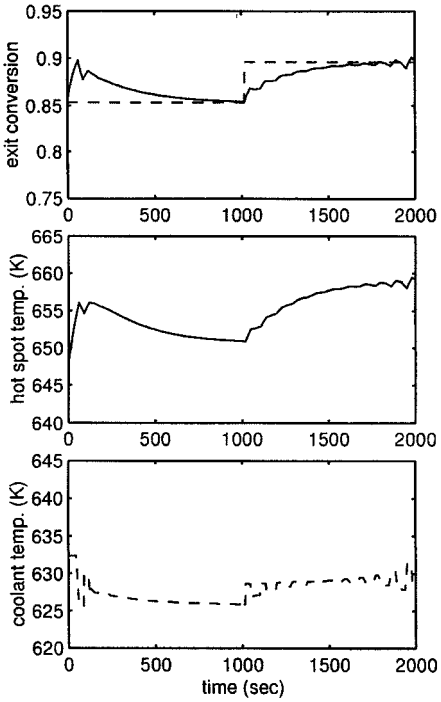

Figure 17. Control performance of single-loop control system after a 5% step increase of exit conversion set point.

—— Response; – – – set point.

same operating conditions are used, it takes some time for exit conversion to approach its steady-state value. Hence, the step change in set point has to be made at 1,000 s, instead of 200 s as in Figure 9. Compared with Figure 9, the closed-loop response of this single-loop control system is much more sluggish. There also appears to be small oscillatory behavior despite parameter adaptation. This may be due to the difficulty of achieving parameter convergence in this system with rapidly changing nonlinear dynamics.

Conclusions

The primary objective of this work was to develop an advanced nonlinear control strategy for exothermic fixed-bed reactors in order to improve control performance. A new nonlinear inferential cascade control strategy for the reactor was presented in this article. An important first step was to partition the entire system into subsystems using a theoretical basis combined with physical insight. A multiple cascade structure was then developed based on this system partitioning approach. This approach allowed the nonlinear controller and the state estimator to be designed based on subsystems, rather than having to deal with the entire system. Thus, this approach extends the applicability of advanced nonlinear control techniques to highly complex processes like fixed-bed reactors, which are described by partial differential equations (PDEs). Moreover, the cascade structure provides some important benefits for control of the fixed-bed reactor such as allowing multiple control objectives, hot-spot position movement, hard constraint handling on both state and control variables, reducing dynamic coupling between loops, and affects of load disturbances. The cascade structure combined with inference of output variables can greatly improve reliability and robustness. Through many closed-loop process control simulations with an industrial phthalic anhydride fixed-bed reactor, it was shown the proposed control strategy can achieve tight control of the exit conversion and stabilization of the hot-spot temperature over a wide range of operation conditions. Its set point tracking and disturbance rejection performance and robustness are excellent, and superior to the single-loop control strategy, where an adaptive GPC was used to design the controller.

The cascade structure can accommodate existing standard or various nonlinear control techniques for the controller design of each subsystem, depending on different characteristics and control requirements. The direct synthesis approach (GMC) was found to be very desirable in designing nonlinear controllers based on subsystems. Using GMC, the control system has some definite advantages such as the direct embedment of the reduced nonlinear process model in the control algorithm, feedforward compensation, and easy tuning.

In general, it is a difficult task to estimate unknown disturbances, states, and outputs of the fixed-bed reactor. This work addressed this practical issue. The partitioning of the system facilitates the estimation of the unknown disturbance, states, and outputs of the fixed-bed reactor. In this work, a composite state and disturbance nonlinear observer was proposed to estimate the unknown temperature states and inlet concentration, and then an output estimator was developed to estimate exit concentration or conversion. Excellent dynamic tracking performance and robustness of the nonlinear

observer against severe model mismatch and measurement errors were demonstrated. Also, the nonlinear observer and output estimator were successfully integrated into the nonlinear inferential cascade control system.

The development of the above nonlinear inferential cascade control strategy was based on a first principle model of the fixed-bed reactor. The model reduction of subsystems was successfully handled based on physical insight and some reasonable assumptions on the fixed-bed reactor. In fact, under the cascade structure, other model reduction approaches (Doyle III et al., 1997) can be used for reducing the model of subsystems. Also, the above nonlinear cascade control concept for exothermic fixed-bed reactors can be extended for the other cases such as when the first principle model of the fixed-bed reactor is not available.

Notation

A = orthogonal collocation matrix
B = orthogonal collocation matrix
C_k = dimensionless concentration of component k ($k = 1, \cdots, m$); C_k^*/C_{ref}
C_p = heat capacity, J/(kg·K)
$E_{k'}$ = activation energy of reaction k' ($k' = 1, \cdots, p$), J/kmol
$(-\Delta H_{k'})$ = heat of reaction k' ($k' = 1, \cdots, p$), J/kmol
$k_{0,k'}$ = reaction rate frequency factor k' ($k' = 1, \cdots, p$), 1/s
K = tuning parameter of GMC controller
L_1, L_2 = gains of observer
L = reactor length, m
m = number of independent component
p = number of reactions
r_0 = reactor radius, m
r_1 = coolant tube radius, m
R_g = gas constant
$R_{k'}$ = dimensionless rate of reaction k' ($k' = 1, \cdots, p$), R^*/R_{ref}
t = dimensionless time; $t^*\upsilon/L$
T = dimensionless bed temperature along the reactor; T^*/T_{ref}
T_c = coolant temperature vector
U = overall heat-transfer coefficient, J/(m^2·s·K)
υ = feed velocity, m/s
z = dimensionless axial distance; z^*/L
ϵ = void volume fraction of reactor
μ = catalyst activity
ρ = density, kg/m^3
λ_e = heat conduction coefficient
τ_p = parameter of lag

Subscripts

a = component A
c = coolant
cr = representative coolant (temperature)
f = fluid
h = hot-spot
in = inlet
I, p = primary
II, s = secondary
III = third
ref = reference
s = solid catalyst
sp = set point

Superscripts

* = real value of reactor variables
$\hat{}$ = estimate, approximate

Literature Cited

Bequette, B. W., "Nonlinear Control of Chemical Processes—A Review," *Ind. Eng. Chem. Res.*, **30**, 1391 (1990).
Brambilla, A., and D. Semino, "Nonlinear Filter in Cascade Control Schemes," *Ind. Eng. Chem. Res.*, **31**, 2694 (1992).
Budman, H. M., C. Webb, T. R. Holcomb, and M. Morari, "Robust Inferential Control for a Packed-bed Reactor," *Ind. Eng. Chem. Res.*, **31**, 1665 (1992).
Clarke, D. W., C. Mohtadi, and P. S. Tuffs, "Generalized Predictive Control: I. The Basic Algorithm: II. Extensions and Interpretations," *Automatica*, **23**, 137 (1987).
Chen, C.-Y., and C.-C. Sun, "Adaptive Inferential Control of Packed-Bed Reactors," *Chem. Eng. Sci.*, **46**, 1041 (1991).
Chidambaram, M., and C. Yugendar, "Model Reference Cascade Control of Nonlinear System: Application to an Unstable CSTR," *Chem. Eng. Commun.*, **113**, 15 (1992).
Cott, B. J., R. G. Durham, P. L. Lee, and G. R. Sullivan, "Process Model-based Engineering," *Comput. Chem. Eng.*, **13**(9), 973 (1989).
Deza, F., E. Busvelle, J. P. Gauthier, and D. Rakotopara, "High Gain Estimation for Nonlinear Systems," *Sys. Control Lett.*, **18**, 295 (1992).
Doyle III, F. J., H. M. Budman, and M. Morari, "'Linearizing' Controller Design for a Packed-bed Reactor using a Low-order Wave Propagation Model," *Ind. Eng. Chem. Res.*, **35**, 3567 (1997).
Farza, M., H. Hammouri, S. Othman, and K. Busawon, "Nonlinear Observers for Parameter Estimation in Bioprocesses," *Chem. Eng. Sci.*, **52**, 4251 (1997).
Finlayson, B. A., *The Model of Weighted Residual and Variational Principles*, Academic Press, New York (1972).
Froment, G. F., "Fixed-bed Catalytic Reaction," *Ind. Eng. Chem.*, **59**, 18 (1967).
Hua, X., M. Mangold, A. Kienle, and E. D. Gilles, "State Profile Estimation of an Autothermal Periodic Fixed-bed Reactor," *Chem. Eng. Sci.*, **53**, 47 (1998).
Jorgensen, S. B., and N. Jensen, "Dynamics and Control of Chemical Reactors—Selectively Surveyed," *DYCORD*, IFAC, New York, 359 (1990).
Jutan, A., J. P. Tremblay, J. F. MacGregor, and J. D. Wright, "Multivariable Computer Control of a Butane Hydrogenolysis: I, II, and III," *AIChE J.*, **23**, 732 (1977).
Kozub, D. J., J. F. MacGregor, and J. D. Wright, "Application of LQ and IMC Controllers to a Packed-bed Reactor," *AIChE J.*, **33**, 1496 (1987).
Kravaris, C., and J. C. Kantor, "Geometric Methods for Nonlinear Process Control: 1. Background; 2. Controller Synthesis," *Ind. Eng. Chem. Res.*, **29**, 2295 (1990).
Kroener, A., P. Holl, W. Marquardt, and E. D. Gilles, "DIVA—An Open Architecture for Dynamic Simulation," *Comput. Chem. Eng.*, **14**, 1289 (1990).
Lee, P. L., and G. R. Sullivan, "Generic Model Control (GMC)," *Comput. Chem. Eng.*, **12**, 573 (1988).
Liu, Z. H., and S. Macchietto, "Partitioning-Space Approach for Nonlinear Process Control," *DYCORD*, IFAC, Copenhagen, 451 (1995).
Ogunnaike, B. A., and W. H. Ray, *Process Dynamics, Modeling and Control*, Oxford University Press, New York (1994).
Soroush, M., "Nonlinear State-observer Design with Application to Reactors," *Chem. Eng. Sci.*, **52**, 387 (1997).
Windes, L. C., and W. H. Ray, "A Control Scheme for Packed Bed Reactors Having a Changing Catalyst Activity Profile: I. On-line Parameter Estimation and Feedback Control," *J. Process Control*, **2**, 23 (1992).
Zeitz, M., "Nonlinear Observers for Chemical Reactors," PhD Thesis in German, VDI-Fortschr.-Ber., Reihe 8, Nr. 27, VDI-Verlag, Duesseldorf (1977).

Appendix A

The dimensionless, normalized model parameters in Eqs. 1–3 are defined as follows

$$Da = \frac{LR_{\text{ref}}}{\upsilon}; \qquad \gamma_{k'} = \frac{E_{k'}}{R_g T_{\text{ref}}} \qquad (k' = 1, \ldots, p);$$

$$\beta = \frac{C_{\text{ref}}}{\rho_f C_{pf} T_{\text{ref}}}; \qquad Le = \frac{(1-\epsilon)\rho_s C_{ps} + \epsilon \rho_f C_{pf}}{\rho_f C_{pf}};$$

$$Pe_h = \frac{\upsilon L \rho_f C_{pf}}{\lambda_{er}}; \qquad \alpha = \frac{2UL}{r_0 \upsilon \rho_f C_{pf}};$$

$$\tau_c = \frac{\upsilon_c}{\upsilon}; \qquad \Omega_c = \frac{2UL}{r' \rho_c C_{pc} \upsilon}; \qquad r' = r_0 \left[\left(\frac{r_0}{r_1} \right)^2 - 1 \right]$$

Appendix B

Consider the following general nonlinear system

$$\dot{x} = f(x,u);\ x(0) = x_o$$
$$y = c^T x. \tag{B1}$$

where x, u, and y are state, input and output (measurement) vector with suitable dimension, respectively; f is a nonlinear function vector, c is a constant vector. To estimate the unknown state x based on known information y and u, we construct the following nonlinear observer

$$\dot{\hat{x}} = f(\hat{x}, u) + L(\hat{x}, u)(y - \hat{y}); \qquad \hat{x}(0) = \hat{x}_0 \tag{B2}$$

where L is an observer gain, which is a nonlinear function matrix with respect to the state and input of the observer. This nonlinear observer design problem is solved by a study of the appropriate differential equations for the errors between the true and the observed process states (Zeitz, 1977).

Introducing the observation error

$$e = \hat{x} - x \tag{B3}$$

The following differential equation results after subtraction of the above Eqs. B1 and B2

$$\dot{e} = \dot{\hat{x}} - \dot{x} = f(\hat{x}, u) - f(x,u) - L(\hat{x}, u) c^T e \tag{B4}$$

Linearization yields

$$\dot{e}\,|_{\hat{x}} = \left(\left. \frac{\partial f}{\partial x} \right|_{\hat{x}} - L(\hat{x}, u) c^T \right) e \tag{B5}$$

If the gain is chosen as

$$L(\hat{x}, u) c^T = \left. \frac{\partial f}{\partial x} \right|_{\hat{x}} + \kappa I \tag{B6}$$

where κ is a positive tuning parameter, the observation error is described by a homogeneous differential equation. When the parameter κ is properly selected, its solution will asymptotically tend to zero for arbitrary initial conditions.

Manuscript received Nov. 18, 1998, and revision received Nov. 12, 1999.